Supporting Information

Exsolution of Metallic Ru Nanoparticles from Defective, Fluorite-type Solid Solutions $Sm_2Ru_xCe_{2-x}O_7$ to Impart Stability on Dry Reforming Catalysts

Muhammad A. Naeem, Paula M. Abdala*, Andac Armutlulu, Sung Min Kim, Alexey Fedorov and Christoph R. Müller*

ETH Zürich, Department of Mechanical and Process Engineering,
Leonhardstrasse 21, 8092 Zurich, Switzerland
* muelchri@ethz.ch (Christoph R. Müller)
* abdalap@ethz.ch (Paula M. Abdala)

Table of Contents

Table S1: Lattice constants determined by the Rietveld refinement of XRD results (λ=0.78956 Å).

Material	Phase	Lattice parameter (a_f) (Å)
$Sm_2Ce_2O_7$	C-type	5.4635(1)*
$Ru/Sm_2Ce_2O_7$-Imp	C-type	5.4626(1)*
	Pyrochlore	5.1352(4)*
$Sm_2Ru_{0.1}Ce_{1.9}O_7$	F-type	5.4587(1)
$Sm_2Ru_{0.2}Ce_{1.8}O_7$	F-type	5.4619(1)
$Sm_2Ru_{0.4}Ce_{1.6}O_7$	F-type	5.4591(1)

*C-type and Pyrochlore lattice parameters (i.e. named in this work as a_c and a_p respectively) are reported as the fluorite cell parameter (i.e., $a_f = \frac{a_c}{2} = \frac{a_p}{2}$).

Table S2: Structural parameters determined from fitted Ru K-edge EXAFS data.

Material	Scattering Path	CN	σ^2 (Å^2)	R (Å)	R-factor	E_0 (eV)
RuO_2	Ru-O	6*	0.002(1)	1.98(1)	0.021	-1(2)
$Sm_2Ru_2O_7$	Ru-O	6.8(8)	0.003(1)	1.99(1)	0.012	-3(2)
	Ru-Sm	4(1)	0.003(1)	3.60(1)	0.012	
	Ru-Ru	4(1)	0.003(1)	3.62(1)	0.012	
$Sm_2Ru_{0.1}Ce_{1.9}O_7$	Ru-O	6(1)	0.006(2)	1.97(2)	0.021	-2(3)
$Sm_2Ru_{0.2}Ce_{1.8}O_7$	Ru-O	6(1)	0.006(2)	1.97(2)	0.023	1(3)
$Sm_2Ru_{0.4}Ce_{1.6}O_7$	Ru-O	6(1)	0.005(2)	1.97(2)	0.019	-1(3)
Ru/$Sm_2Ce_2O_7$-Imp	Ru-O	6.7(8)	0.003(1)	1.98(1)	0.036	-2(2)
	Ru-Sm	3(1)	0.003(1)	3.54(2)	0.036	
	Ru-Ru	3(1)	0.003(1)	3.56(2)	0.036	
$Sm_2Ru_{0.2}Ce_{1.8}O_7$ (re-oxid@700°C_Air; 2cycle)	Ru-O	6(1)	0.006(2)	1.97(2)	0.022	-1(3)
Ru foil	Ru-Ru	12(1)	0.004(1)	2.70(1)	0.008	4(1)
$Sm_2Ru_{0.2}Ce_{1.8}O_7$ (red@700°C_H_2)	Ru-Ru	6(1)	0.008(1)	2.61(1)	0.021	1(2)
$Sm_2Ru_{0.2}Ce_{1.8}O_7$ (red@800°C_DRM)	Ru-Ru	6.5(9)	0.007(1)	2.67(5)	0.003	-6(1)
Ru/$Sm_2Ce_2O_7$-Imp (red; 700°C_H_2)	Ru-Ru	10(1)	0.005(1)	2.67(5)	0.004	4(1)
$Sm_2Ru_{0.2}Ce_{1.8}O_7$ (Post DRM)	Ru-Ru	7(1)	0.008(1)	2.62(1)	0.018	2(1)
Ru/$Sm_2Ce_2O_7$-Imp (Post DRM)	Ru-Ru	11(1)	0.005(1)	2.67(1)	0.011	5(1)

*Fixed to the crystallographic values during the fitting. The values in parenthesis are the standard deviation obtained in the fittings.

Table S3: Structural parameters determined from fitted EXAFS data on Ce and Sm K-edges.

Material	Fitting parameters	Ce K-edge		Sm K-edge	
	Scattering Path	Ce-O	Ce-M	Sm-O	Sm-M
$Sm_2Ru_{0.05}Ce_{1.95}O_7$	**CN**	8.4(8)	7(1)	7.8(9)	8(2)
	σ^2 (Å^2)	0.011(1)	0.009(2)	0.010(1)	0.013(2)
	R (Å)	2.29(1)	3.78(1)	2.37(1)	3.77(3)
	E_0	-4(1)		-2(1)	
	R-factor	0.013		0.021	
$Sm_2Ru_{0.2}Ce_{1.8}O_7$	**CN**	8.3(8)	6(1)	7.3(9)	7(3)
	σ^2 (Å^2)	0.012(1)	0.009(1)	0.010(1)	0.011(2)
	R (Å)	2.29(1)	3.73(1)	2.37(1)	3.78(1)
	E_0 (eV)	-4(1)		-2(1)	
	R-factor	0.012		0.025	
$Sm_2Ru_{0.4}Ce_{1.6}O_7$	**CN**	8.3(8)	5(1)	7.1(8)	6(2)
	σ^2 (Å^2)	0.012(1)	0.008(1)	0.009(1)	0.010(2)
	R (Å)	2.29(1)	3.77(1)	2.36(1)	3.78(1)
	E_0 (eV)	-4(1)		-2(1)	
	R-factor	0.013		0.021	
CeO_2	**CN**	8*	12*		
	σ^2 (Å^2)	0.006(1)	0.004(2)		
	R (Å)	2.34(1)	3.85(1)		
	E_0 (eV)	-3(1)			
	R-factor	0.017			

*Fixed to the crystallographic values during the fitting. The values in parenthesis are the standard deviation obtained in the fittings.

EXAFS analysis: The EXAFS fitting of the extended X-ray absorption fine structure (EXAFS) data were performed using the Artemis software. The fits of the first (Ce-O, Sm-O) and second (Ce-M, Sm-M) coordination shells (where M is Ce, Sm or Ru), allowed to determine the average coordination numbers (CN), Debye-Waller factors σ^2, and interatomic distances for each sphere. The fittings were performed in R space for k weight = 2 and 3, k range = 2–12 Å^{-1} for Ce K-edge and 2.7–12 Å^{-1} for Sm K-edge, dk =1 and R = 1.3–3.9 Å, dr = 0.3 (S_0 = 1, determined from CeO_2 standard). For the Ru K-edge, Ru-O, Ru-Sm and Ru-Ru shells were fitted for $Sm_2Ru_2O_7$, Ru/$Sm_2Ce_2O_7$-Imp samples, Ru-O for $Sm_2Ru_xCe_{2-x}O_7$ and RuO_2, and Ru-Ru for the reduced materials. The following parameters were used: k weight = 2 and 3 k range = 3-12 Å^{-1}, R range = 1-2.1 Å, dk = 1, dr = 0.5 (S_0 = 0.82, determined from Ru foil).

Table S4: Physicochemical properties of synthesized materials after reduction at 700 °C in 5 vol% H_2/Ar (1 h) by hydrogen temperature-programmed desorption (H_2-TPD)

Catalyst	H_2 uptake[a)] [µmol/g]	Ru content[b)] [wt.%]	Ru(0) dispersion [%]	Ru(0) particle size [nm]
$Sm_2Ru_{0.1}Ce_{1.9}O_7$	51	1.5	69%	1.9
$Sm_2Ru_{0.2}Ce_{1.8}O_7$	96	3.0	65%	2.0
$Sm_2Ru_{0.4}Ce_{1.6}O_7$	137	6.0	46%	2.9
$Ru/Sm_2Ce_2O_7$-Imp	38	3.0	26%	5.2

a): H_2 uptake was measured by H_2-TPD

b): Nominal Ru loading

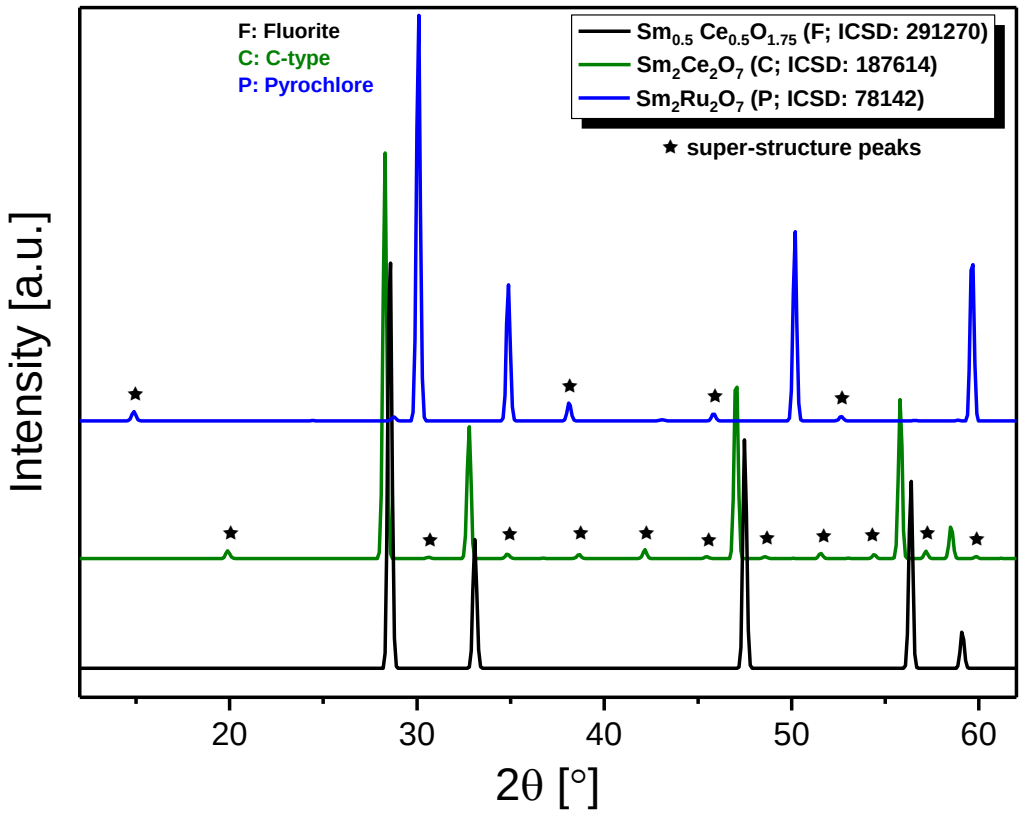

Figure S1: (a) Comparison of the simulated XRD pattern of fluorite, C-type and pyrochlore structures (Inorganic Crystal Structure Database).

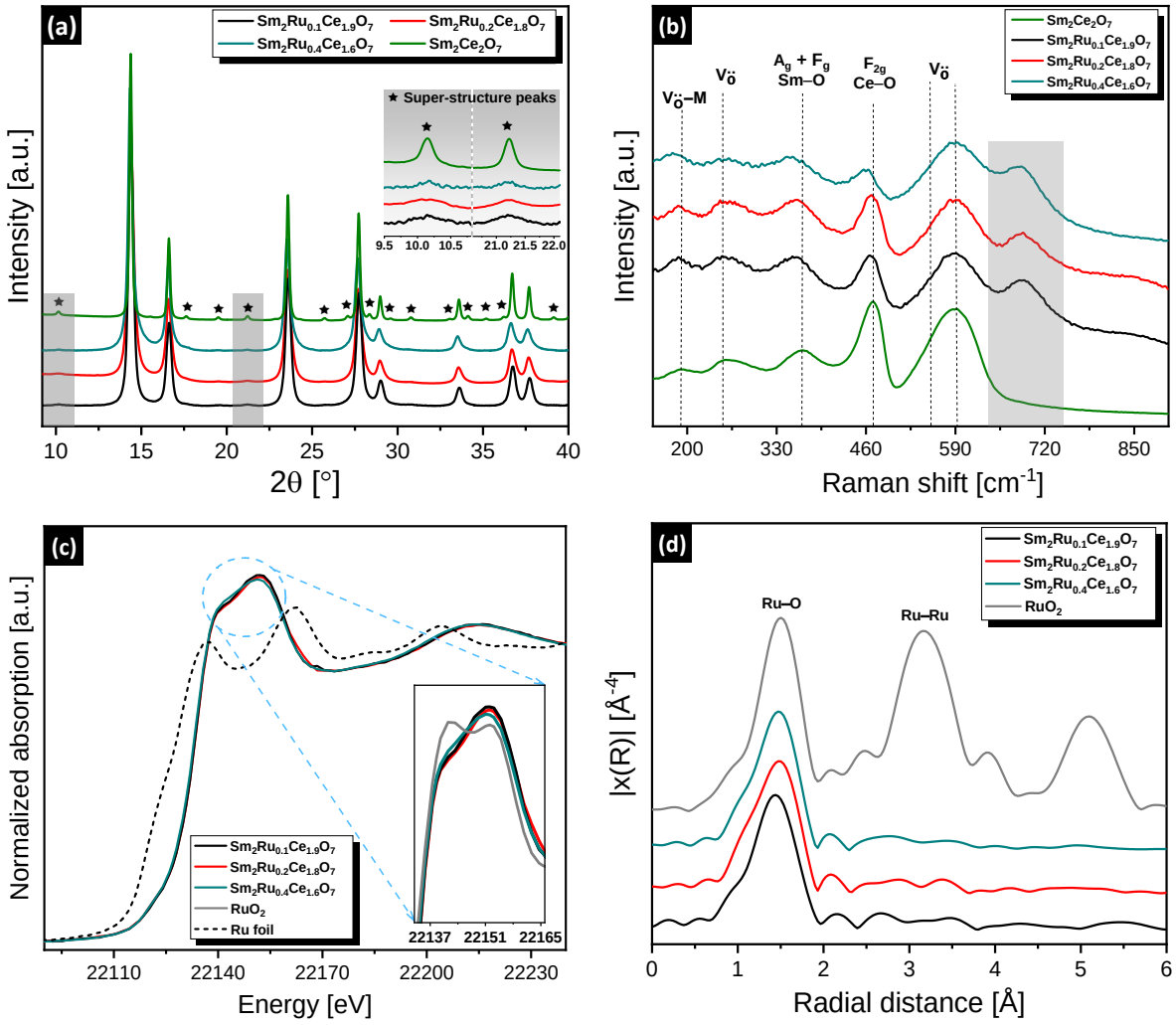

Figure S2: (a) XRD patterns (λ= 0.78956 Å), (b) Raman spectra, (c) normalized Ru K-edge XANES spectra and (c, d) Fourier transform (FT) of k^3-weighted EXAFS data, for $Sm_2Ru_xCe_{2-x}O_7$ (x = 0, 0.1, 0.2, 0.4).

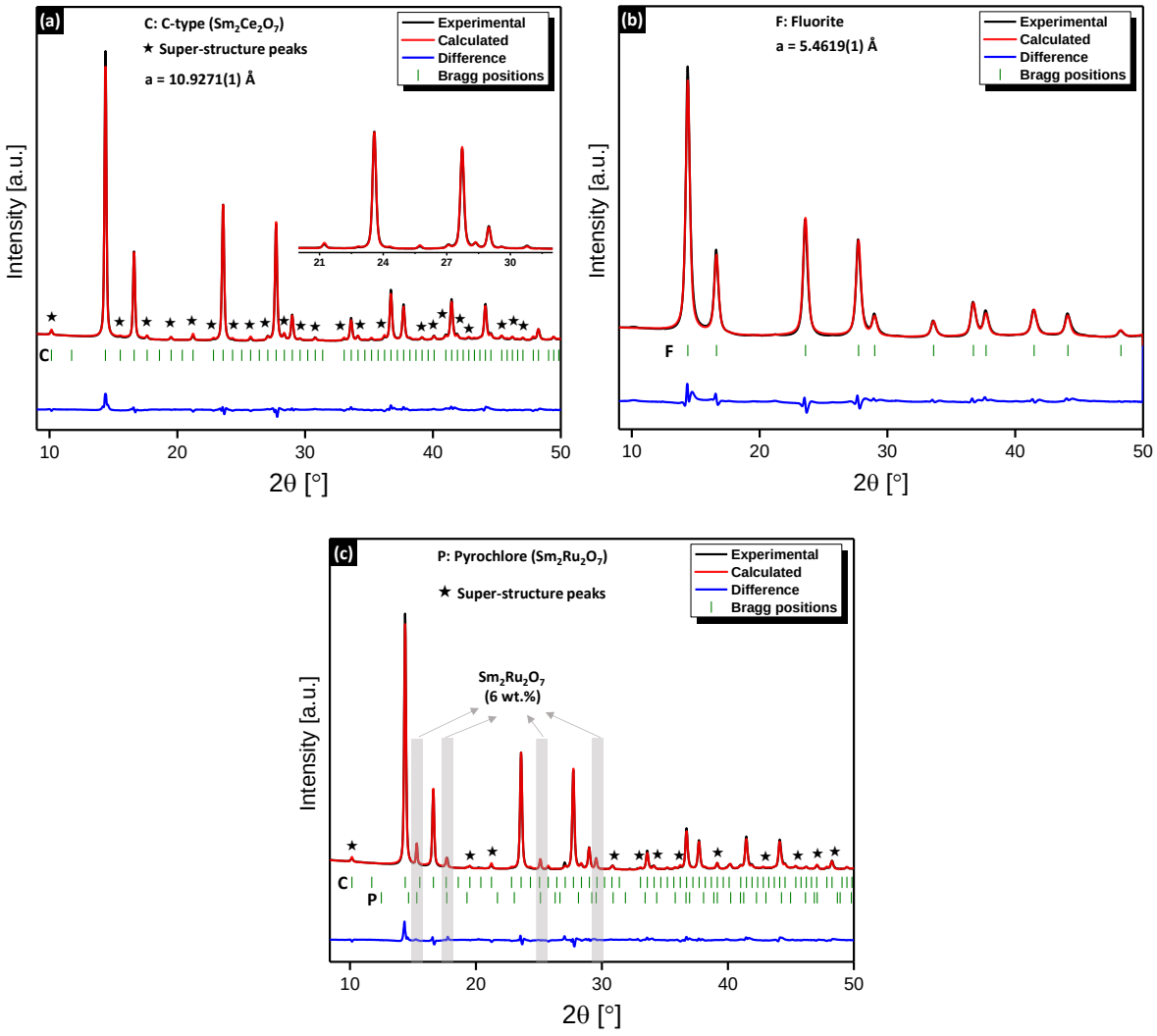

Figure S3: Rietveld refinement plots for (a) $Sm_2Ce_2O_7$, (b) $Sm_2Ru_{0.2}Ce_{1.8}O_7$ and (c) $Ru/Sm_2Ce_2O_7$-Imp catalysts calcined at 800 °C (λ=0.78956 Å).

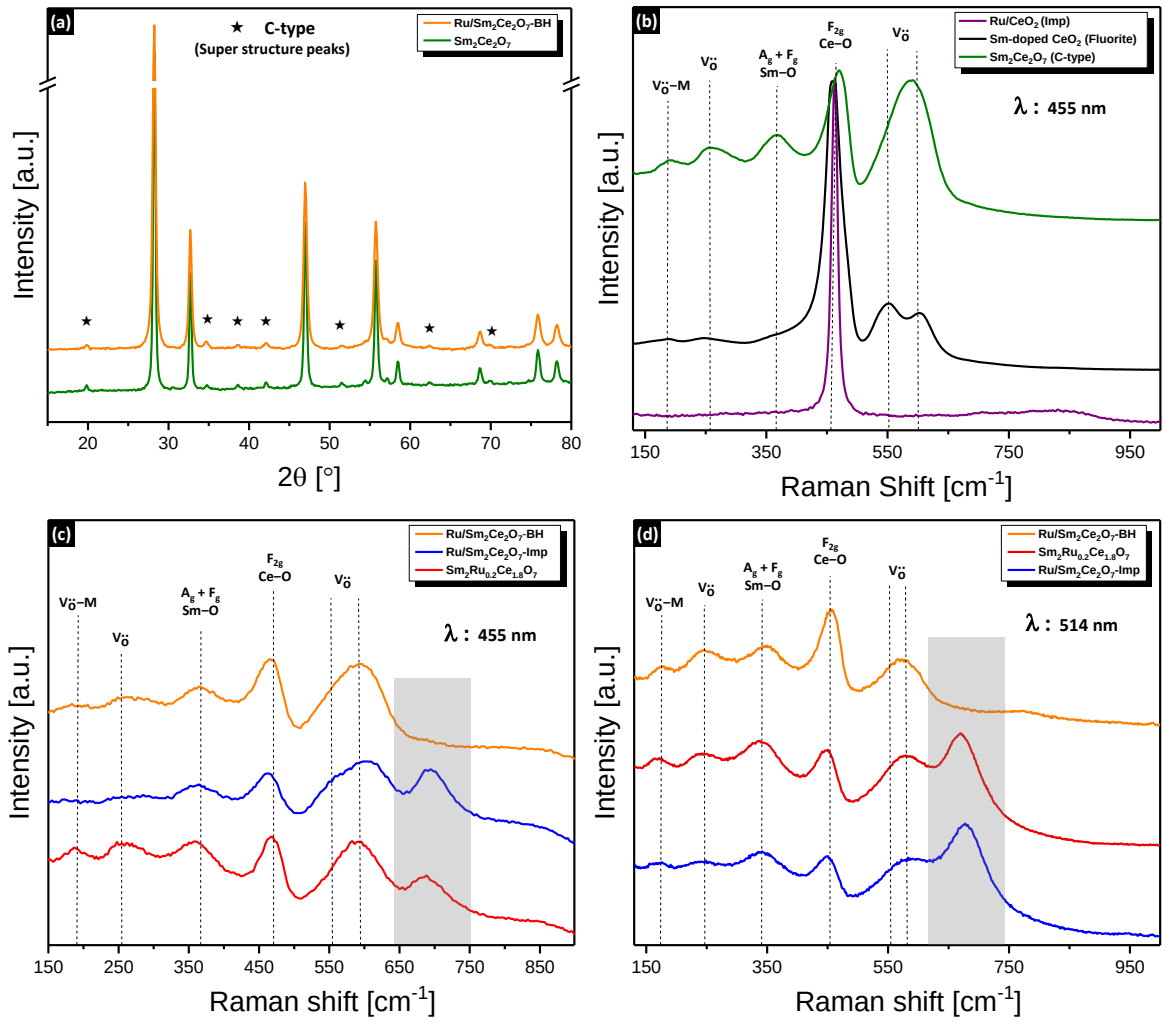

Figure S4: (a) XRD patterns (λ=1.54056 Å) of $Sm_2Ce_2O_7$ and Ru/$Sm_2Ce_2O_7$-BH materials, respectively. (b) Raman spectra (laser excitation: 455 nm) of Ru/CeO_2-Imp, $Sm_2Ce_2O_7$, and Sm doped (20%) CeO_2. (c, d) Raman spectra (laser excitation: 455 and 514 nm, respectively) of Ru/$Sm_2Ce_2O_7$-Imp, Ru/$Sm_2Ce_2O_7$-BH, and $Sm_2Ru_{0.2}Ce_{1.8}O_7$ with the assignment of bands.

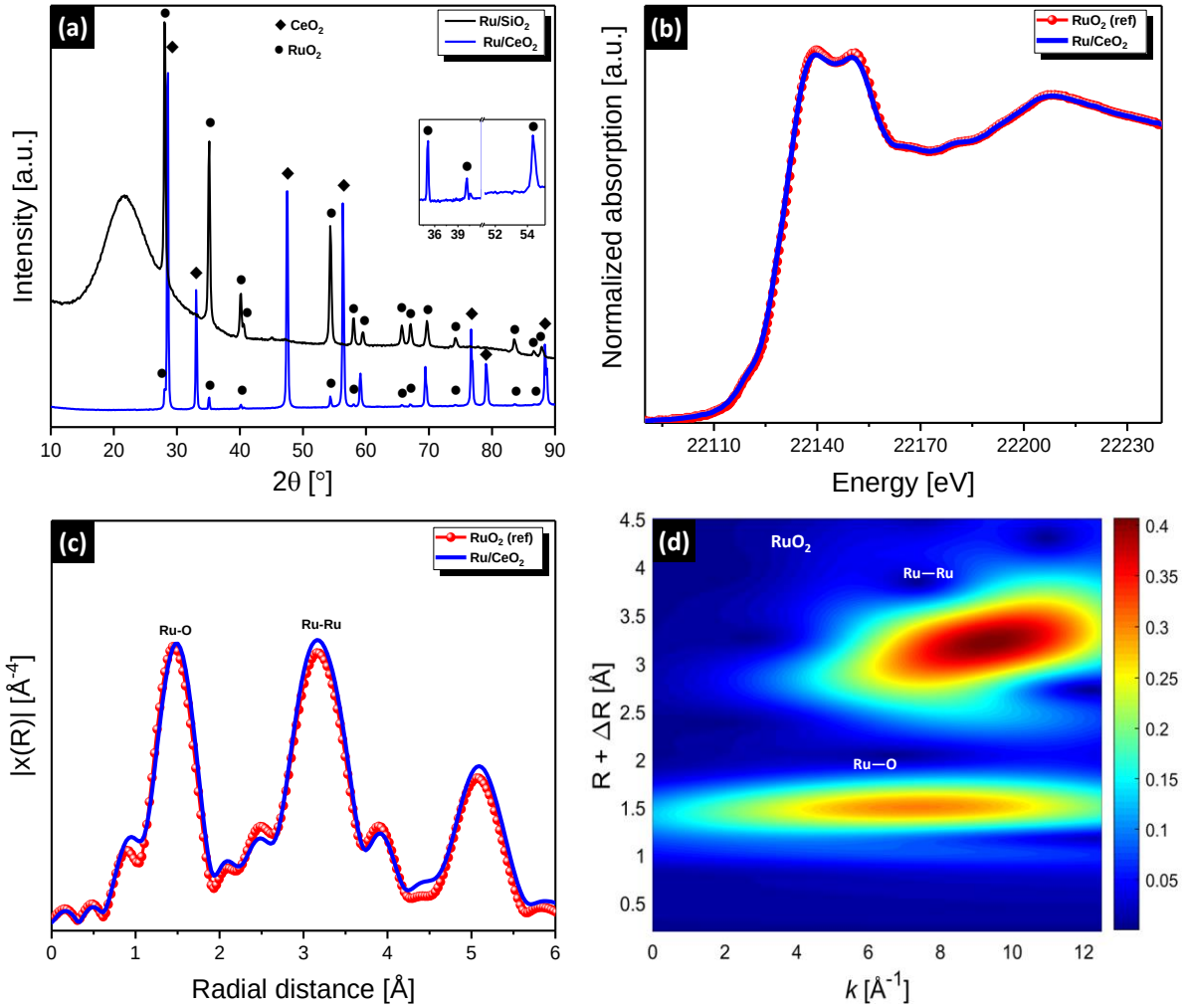

Figure S5: XRD pattern of Ru/SiO_2 and Ru/CeO_2-Imp materials calcined at 800 °C. (b, c) Normalized Ru K-edge XANES spectra and FT of k^3-weighted EXAFS data for Ru/CeO_2-Imp calcined at 800 °C, respectively. (d) WT of k^3-weighted EXAFS data for RuO_2.

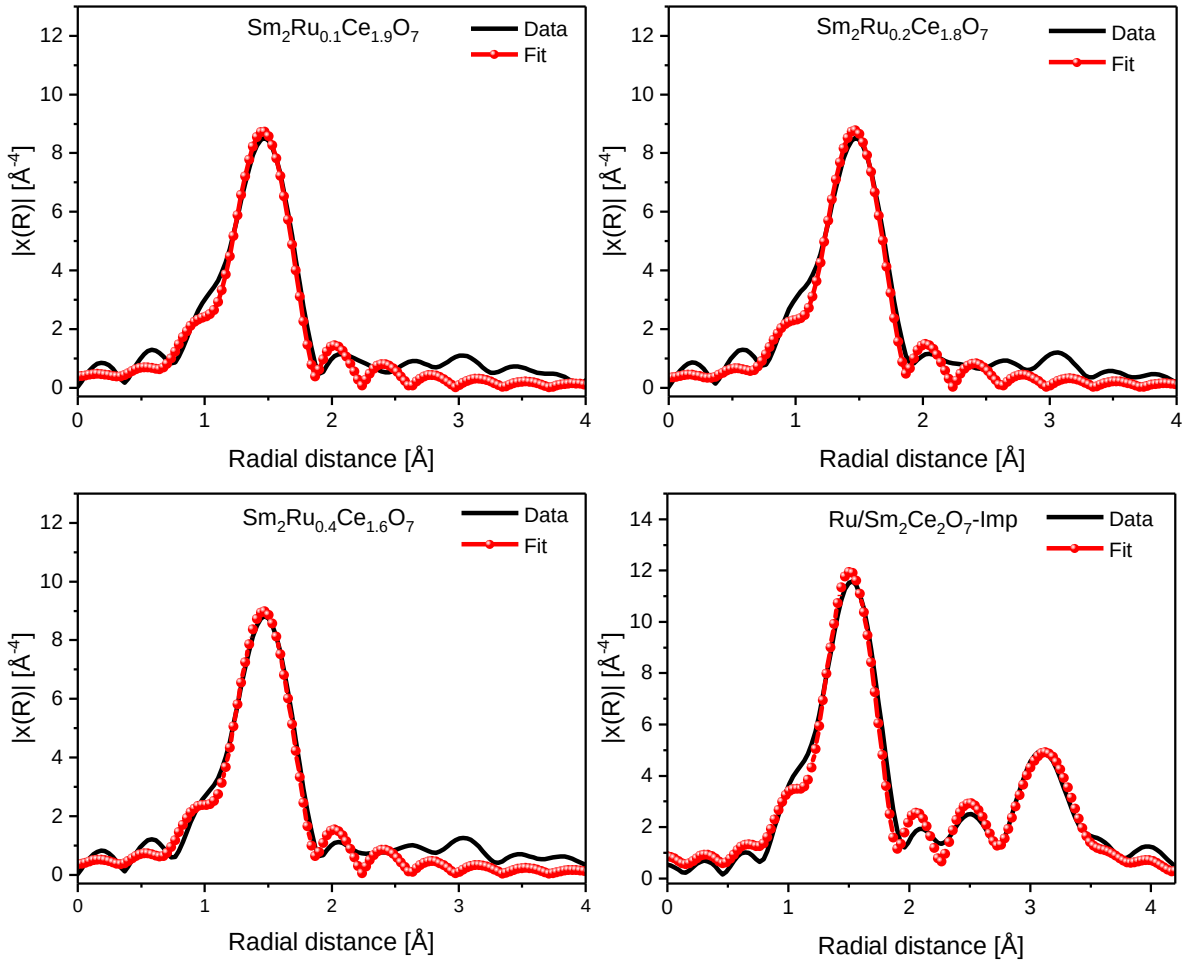

Figure S6a: Fitting of Ru K-edge k^3-weighted EXAFS data of $Sm_2Ru_xCe_{2-x}O_7$ (x = 0, 0.1, 0.2, 0.4) and $Ru/Sm_2Ce_2O_7$-Imp, respectively.

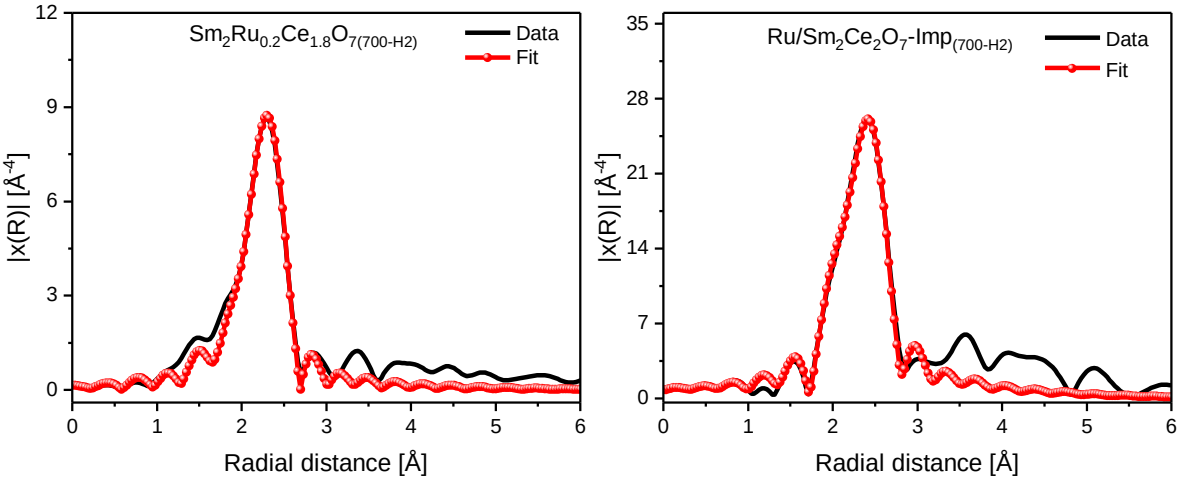

Figure S6b: Fitting of Ru K-edge k^3-weighted EXAFS data of $Sm_2Ru_{0.2}Ce_{21.8}O_{7(700\text{-}H2)}$ and $Ru/Sm_2Ce_2O_7$-Imp(700-H_2) materials after reductive treatment at 700 °C in 10 vol% H_2 in He (10 mL min^{-1}, 1 h).

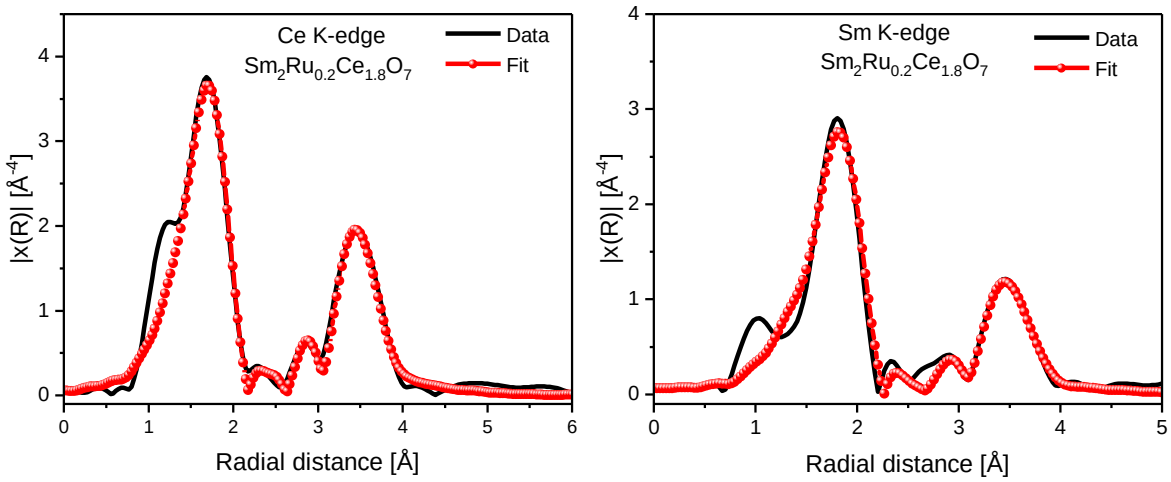

Figure S6c: Fitting of Ce and Sm K-edge k^3-weighted EXAFS data for $Sm_2Ru_{0.2}Ce_{21.8}O_7$.

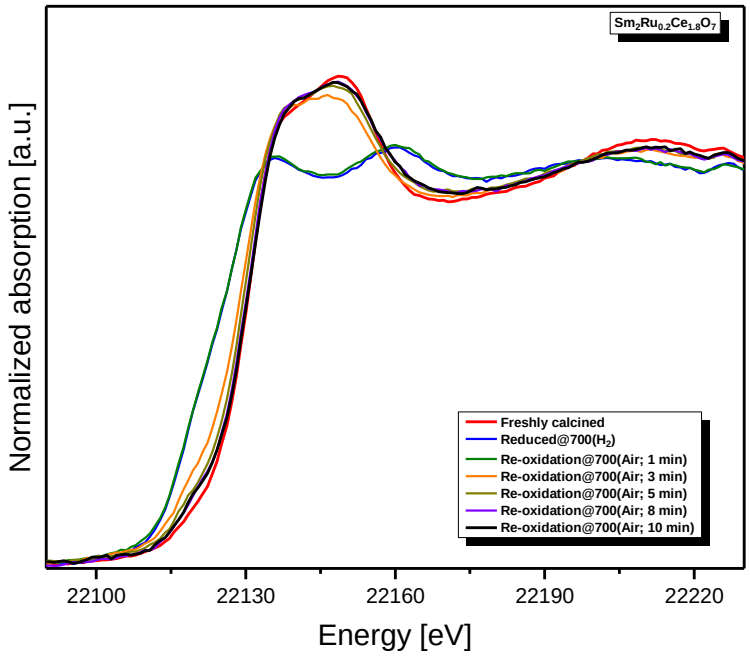

Figure S6d: Normalized in situ Ru K-edge XANES spectra for $Sm_2Ru_{0.2}Ce_{1.8}O_{7(700\text{-}H2)}$ during re-oxidation at 700 °C. The reduction and re-oxidation was performed in 10 vol% H_2 in He and 20 vol% O_2 in He, respectively.

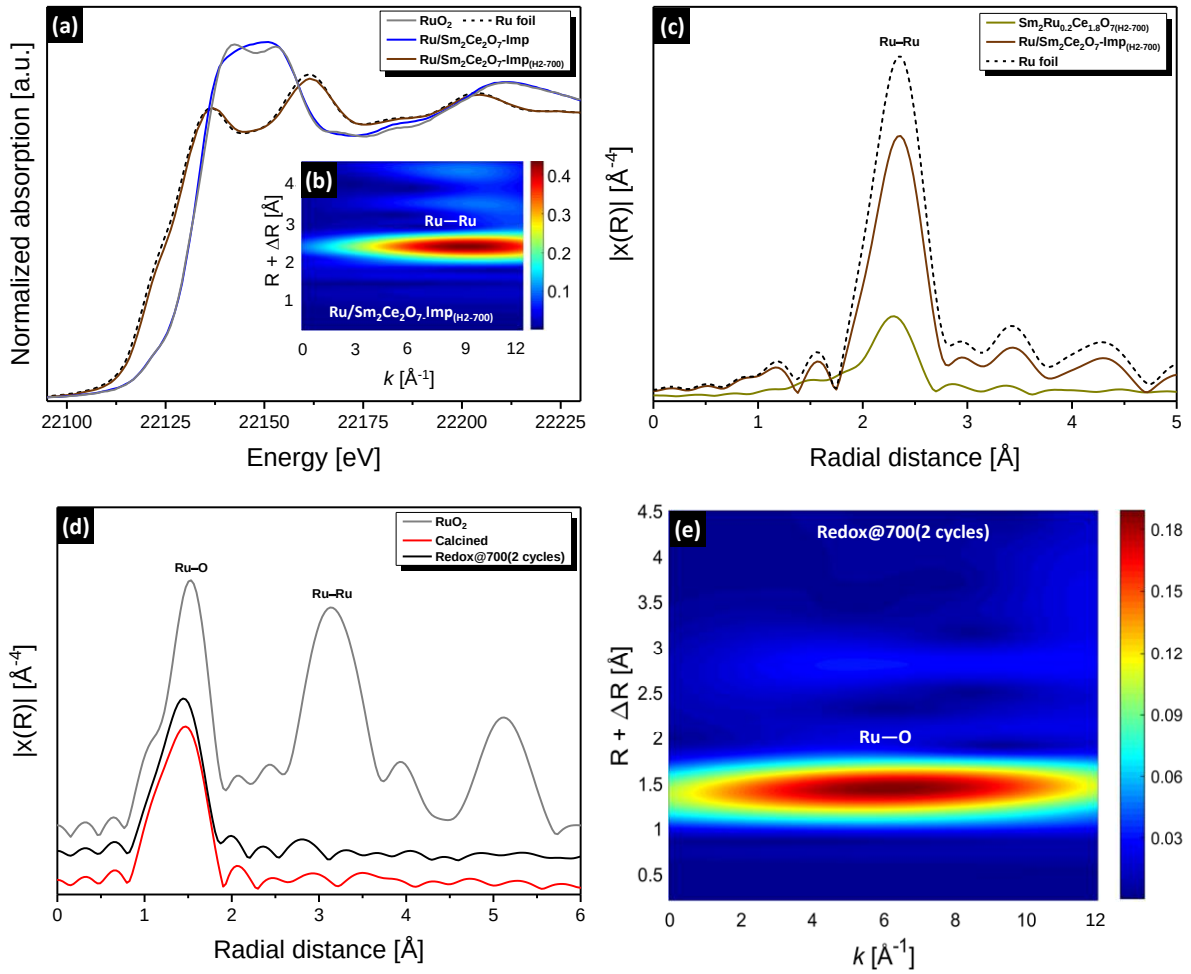

Figure S7: (a) Normalized in situ Ru K-edge XANES spectra of Ru/$SmCe_2O_7$-Imp before and after H_2-treatment (10 vol% H_2 in He) at 700 °C. (b) WT of k^3-weighted EXAFS signals for Ru/$SmCe_2O_7$-$Imp_{(H2\text{-}700)}$. (c) Comparison of FT-EXAFS patterns of $Sm_2Ru_{0.2}Ce_{1.8}O_{7(H2\text{-}700)}$ and Ru/$Sm_2Ce_2O_7$-$Imp_{(H2\text{-}700)}$ with a Ru foil. (d) FT and (e) WT of k^3-weighted EXAFS data for $Sm_2Ru_{0.2}Ce_{1.8}O_7$ after two redox cycles at 700 °C (after oxidative treatment). The reduction and re-oxidation was performed in 10 vol% H_2 in He and 20 vol% O_2 in He, respectively.

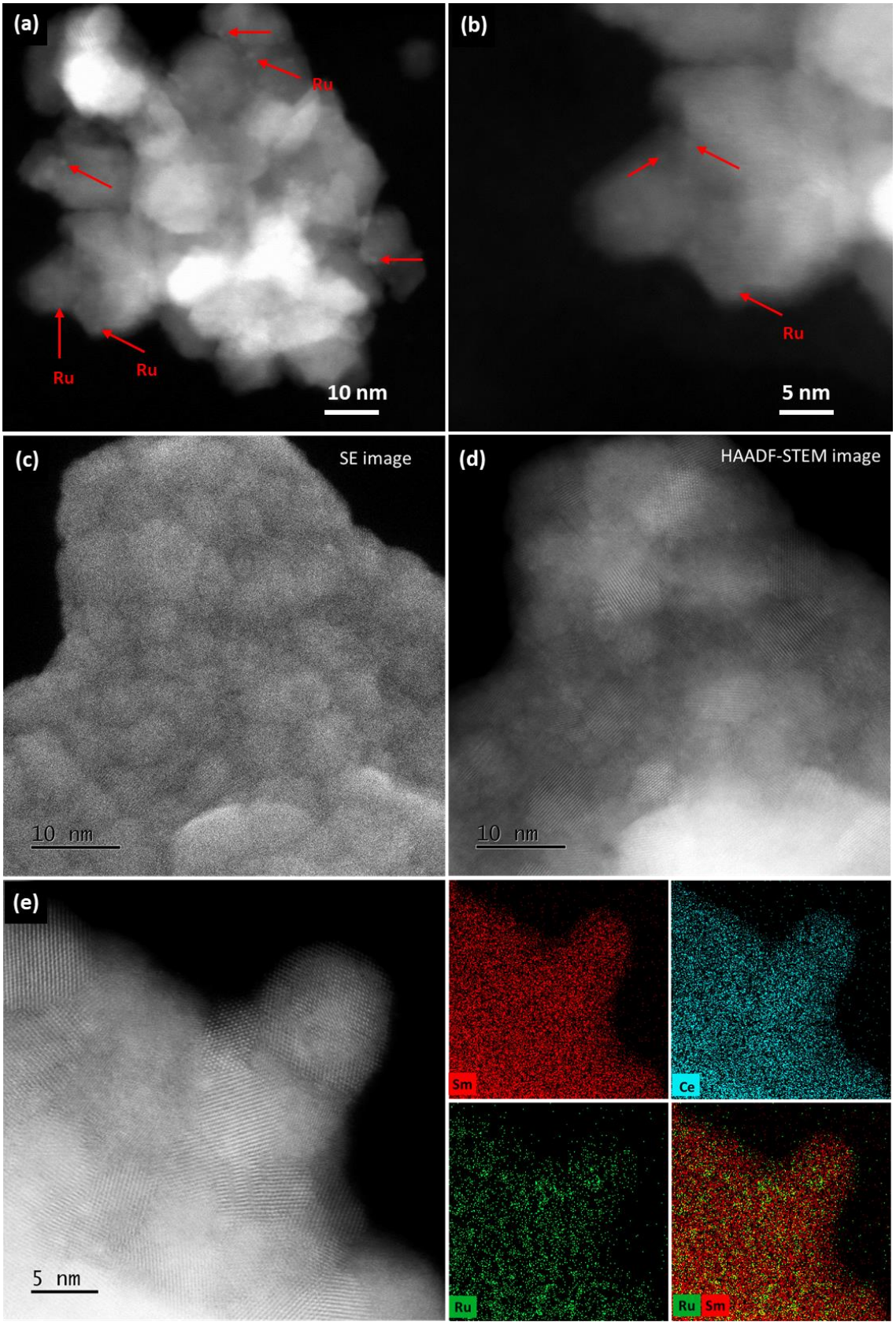

Figure S8: High resolution STEM-EDX images of the reduced $Sm_2Ru_{0.2}Ce_{1.8}O_{7(700\text{-}H2)}$ material.

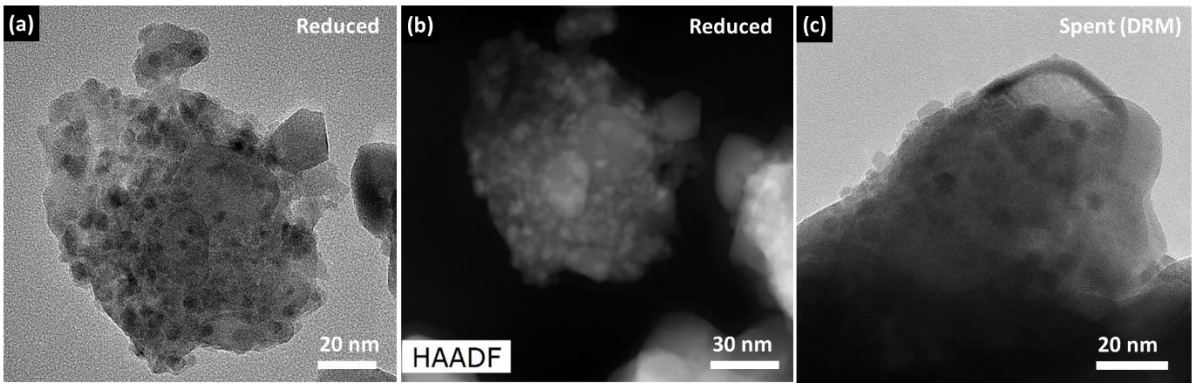

Figure S9: TEM and STEM images of the ex situ prepared reduced Ru/$Sm_2Ce_2O_7$-$Imp_{(700\text{-}H2)}$ (a-b) and spent Ru/$Sm_2Ce_2O_7$-Imp tested at 700 °C for 48 h on TOS (c).

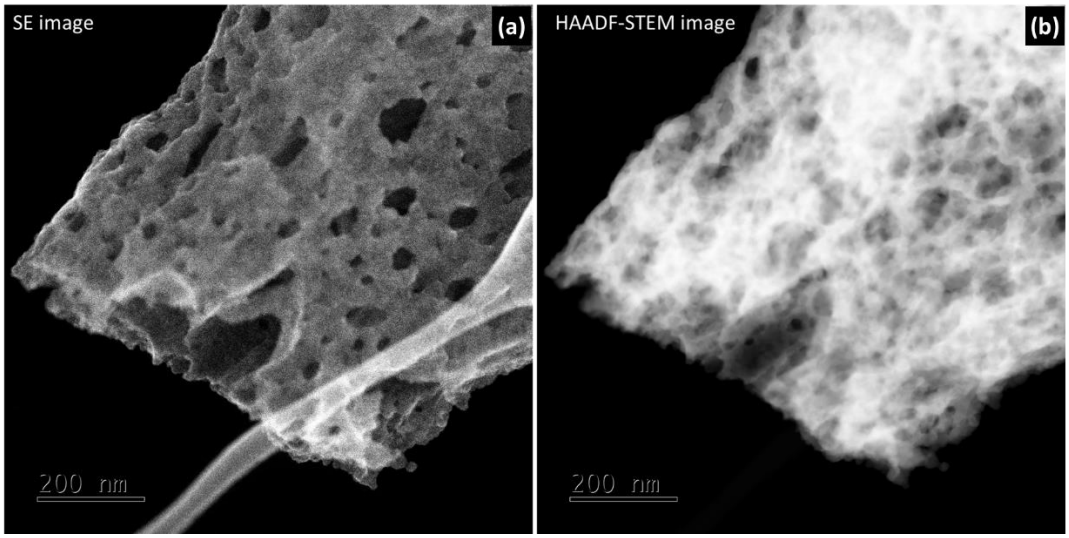

Figure S10: SE and STEM images of the reduced $Sm_2Ru_{0.2}Ce_{1.8}O_{7(700\text{-}H2)}$.

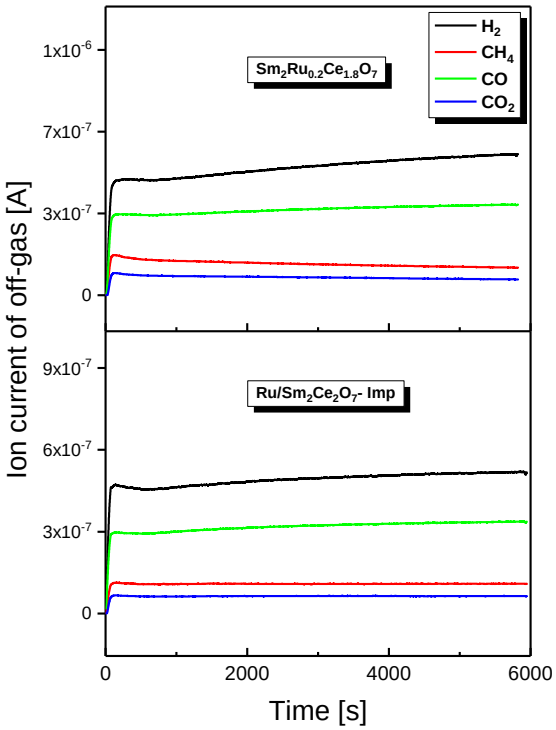

Figure S11: Mass spectrometer (MS) signal of the off-gas for $Sm_2Ru_{0.2}Ce_{1.8}O_7$ and $Ru/Sm_2Ce_2O_7$-Imp during an operando DRM (XAS-XRD) experiment (Temp: 700 °C; $CH_4 : CO_2 : He$ = 3:3:3 mL min^{-1}). Prior to performing the operando DRM test, each catalyst was reduced in situ in 10 vol% H_2 in He at 700 °C.

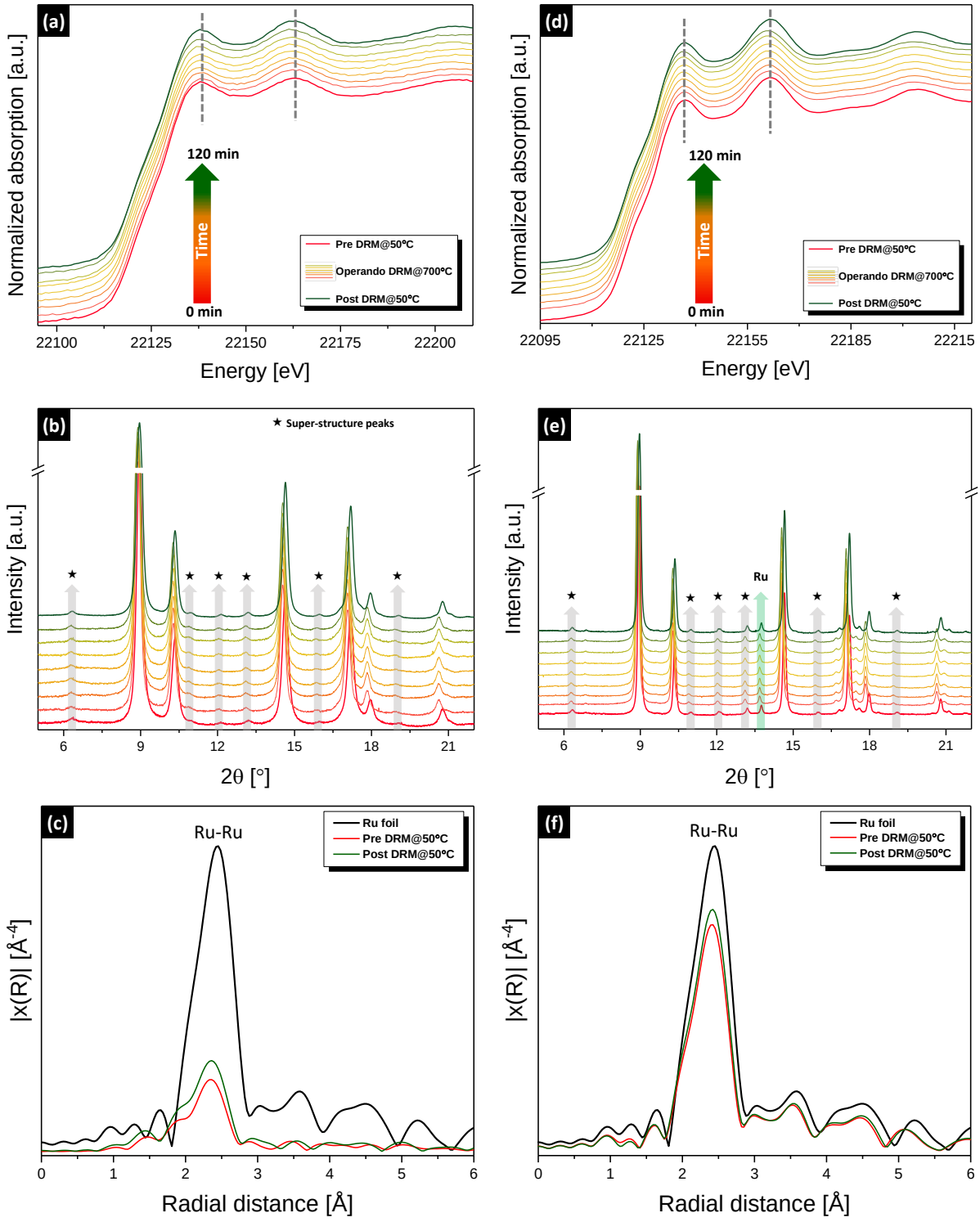

Figure S12: Combined XAS (Ru K-edge)-XRD results of (a-b) $Sm_2Ru_{0.2}Ce_{1.8}O_7$ and (d-e) $Ru/Sm_2Ce_2O_7$-Imp under operando DRM conditions ($CH_4 : CO_2 : He = 3 : 3 : 3$ mL min^{-1}; 700 °C), respectively. FT-EXAFS data collected at 50°C before and after operando DRM and after reductive treatment on (c) $Sm_2Ru_{0.2}Ce_{1.8}O_7$ and (d) $Ru/Sm_2Ce_2O_7$-Imp catalysts. Prior to performing the operando DRM test, each catalyst was reduced in situ in 10 vol% H_2 in He at 700 °C and cooled down to 50°C in order to collect EXAFS data (to reduce thermal vibration effects in the EXAFS).

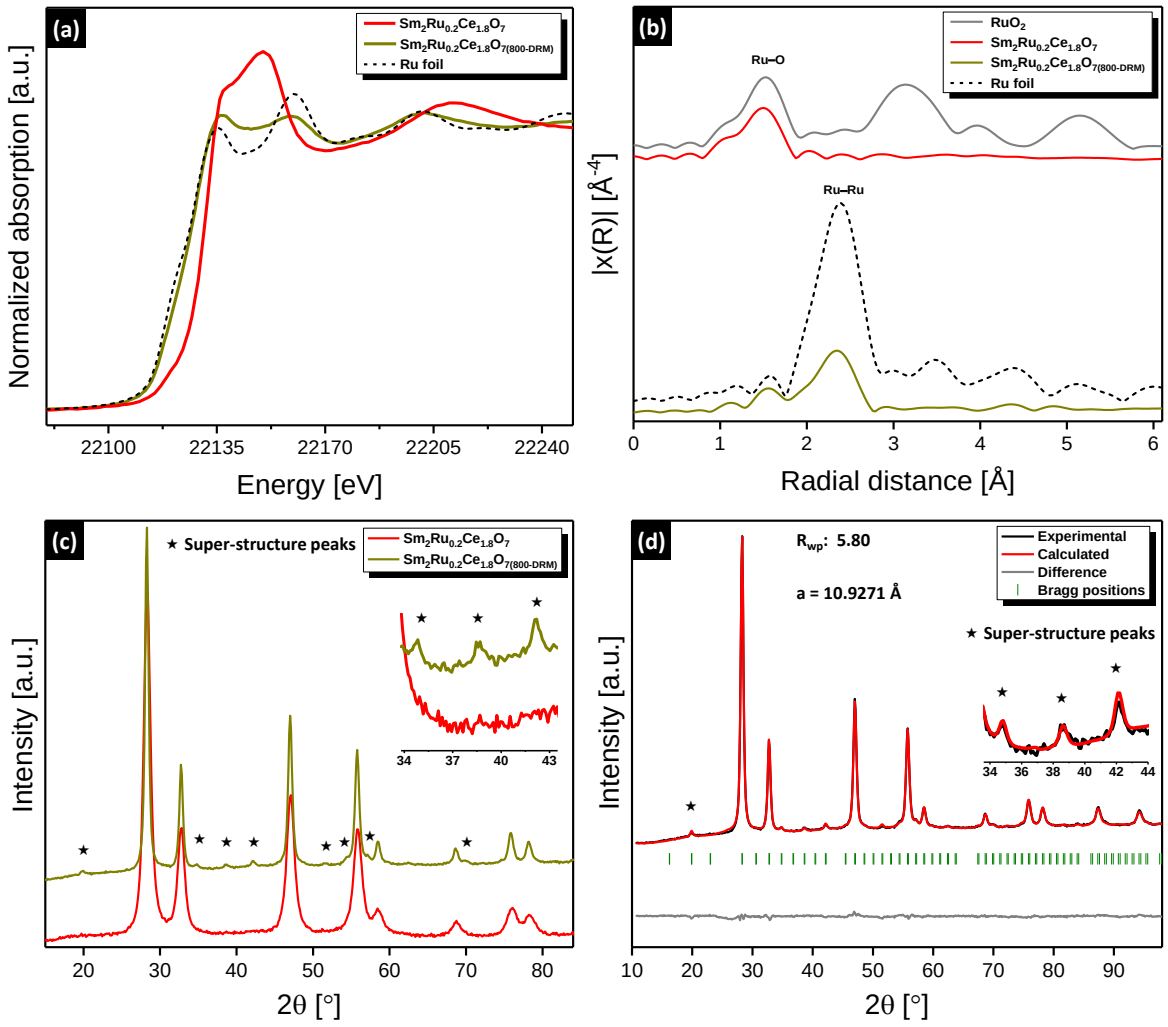

Figure S13: (a) Normalized ex situ Ru K-edge XANES spectra and (b) Fourier transforms of the k^3-weighted EXAFS data of freshly calcined $Sm_2Ru_{0.2}Ce_{1.8}O_7$ and $Sm_2Ru_{0.2}Ce_{1.8}O_{7(800\text{-}DRM)}$ treated by a DRM reaction mixture ; (c,d) Rietveld refinement of $Sm_2Ru_{0.2}Ce_{1.8}O_{7(800\text{-}DRM)}$ (λ=1.54056 Å).

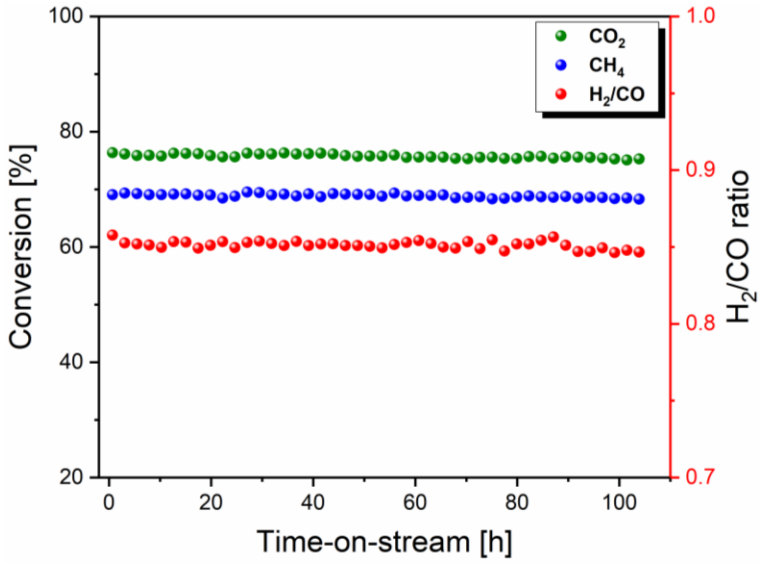

Figure S14: Conversion of CH_4 and CO_2 and H_2/CO versus time-on-stream of $Sm_2Ru_{0.2}Ce_{1.8}O_7$ for the DRM at 700° C (SV: 60 $L \cdot g_{cat}^{-1} \cdot h^{-1}$). Prior to acquiring the activity data the catalyst was reduced in a DRM reaction mixture at 800 °C for 1 h.

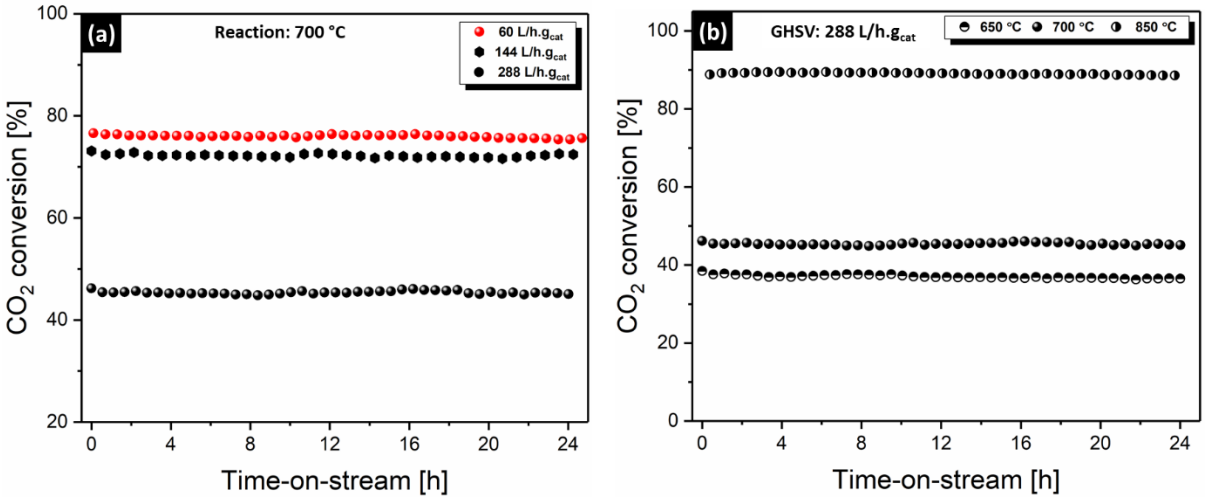

Figure S15: (a) Effect of space velocity (SV) ($L \cdot g_{cat}^{-1} \cdot h^{-1}$) at a fixed reaction temperature (i.e., 700 °C) on CO_2 conversion and (b) effect of the reaction temperature at a fixed SV (i.e., 288 $L \cdot g_{cat}^{-1} \cdot h^{-1}$) on the catalytic performance of $Sm_2Ru_{0.2}Ce_{1.8}O_7$ catalyst on CO_2 conversion with time-on-stream. Prior to acquiring the activity data, the catalyst was reduced in the DRM reaction mixture at 800 °C for 1 h.

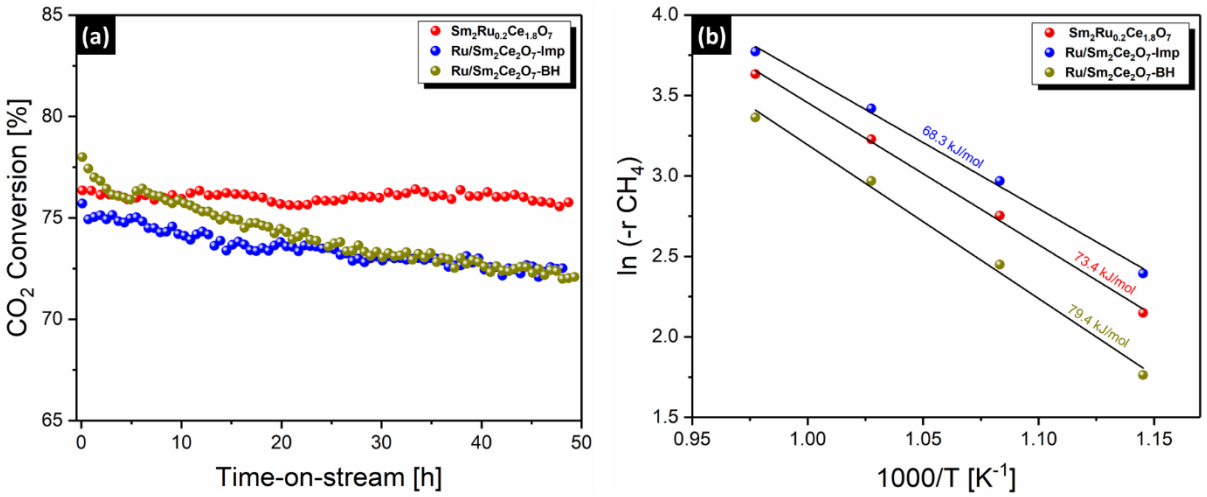

Figure S16: (a) CO_2 conversions versus time-on-stream for the synthesized catalysts (700 °C; SV = 60 L g_{cat}^{-1} h^{-1}). (b) Arrhenius plot constructed using CH_4 conversion rates over Ru-based catalysts (1 atm; 600-750 °C; SV = 288 L g_{cat}^{-1} h^{-1}). Prior to acquiring the activity data, each catalyst was reduced in the DRM reaction mixture at 800 °C for 1 h.

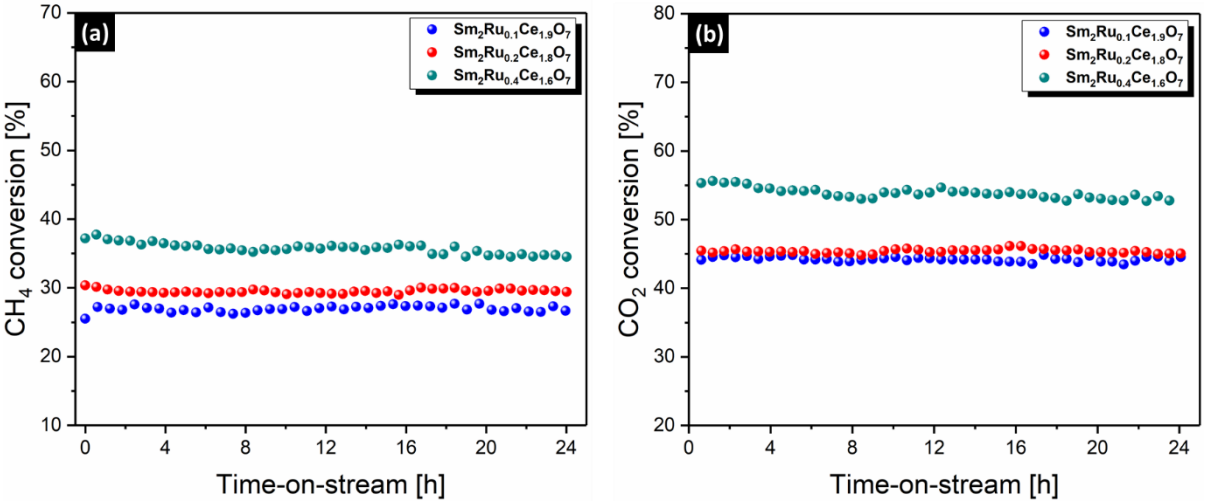

Figure S17: Conversion versus time-on-stream of (a) CH_4 and (b) CO_2 under DRM conditions at 700° C (1 atm, SV: 288 L·g_{cat}^{-1}·h^{-1}) for $Sm_2Ru_xCe_{2-x}O_7$ (x = 0.1, 0.2, 0.4) catalysts. Prior to acquiring the activity data, each catalyst was reduced with a DRM reaction mixture at 800 °C for 1 h.

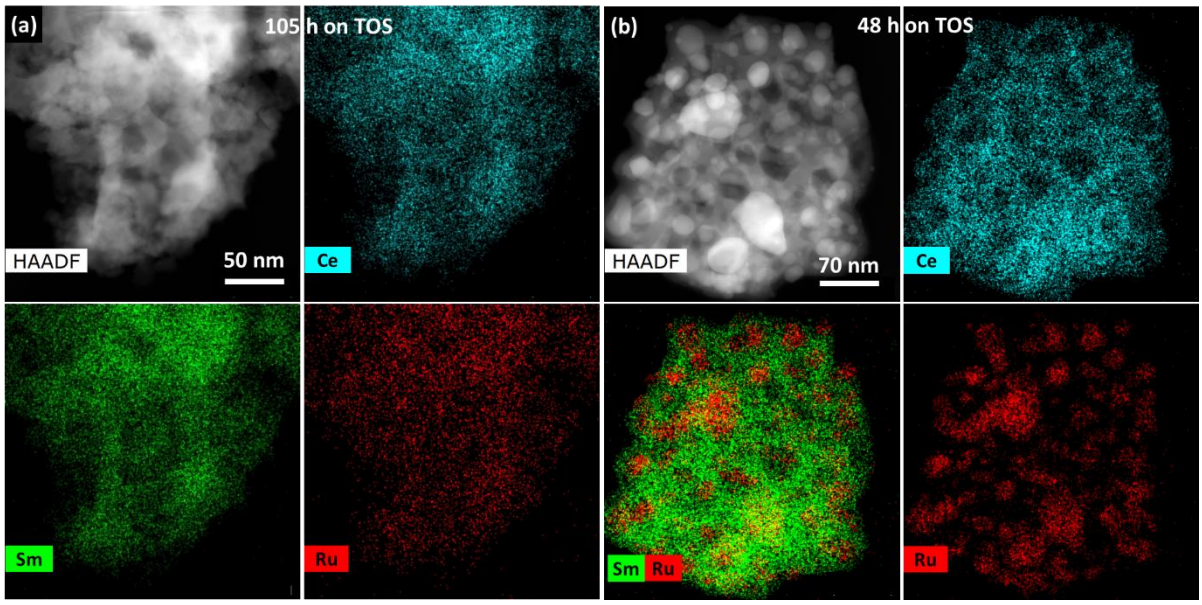

Figure S18: STEM-EDX images of spent (a) $Sm_2Ru_{0.2}Ce_{1.8}O_7$ and (b) $Ru/Sm_2Ce_2O_7$-BH tested at 700 °C (SV = 60 L g_{cat}^{-1} h^{-1}) after 105 h and 48 h on TOS, respectively.

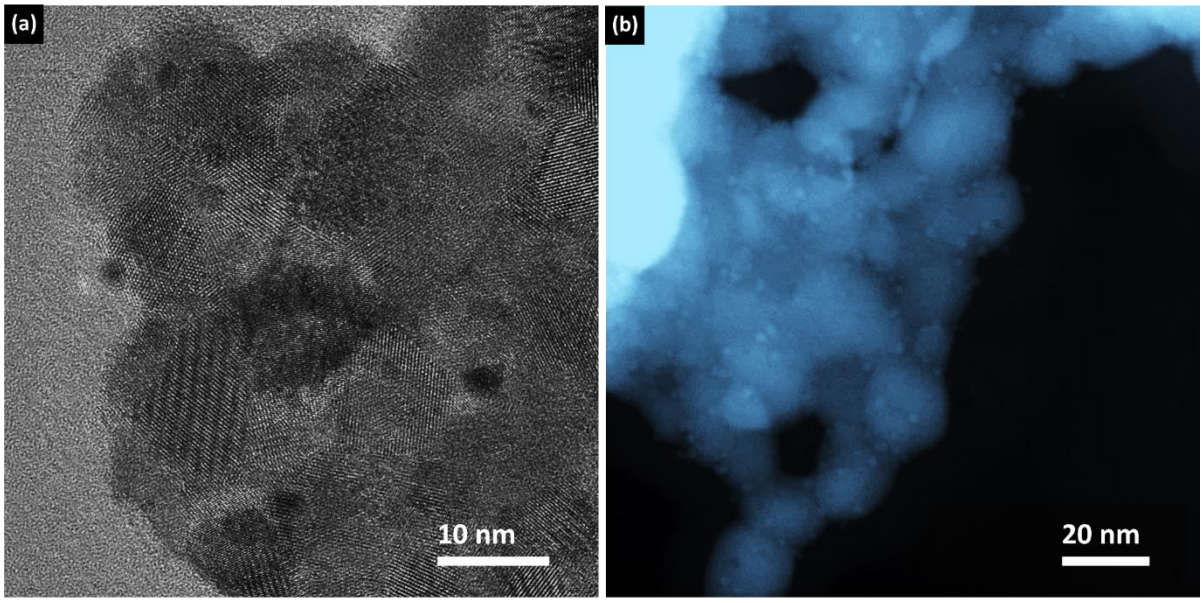

Figure S19: TEM and STEM images of spent $Sm_2Ru_{0.4}Ce_{1.6}O_7$; tested for 24 h under DRM conditions at 700 °C.

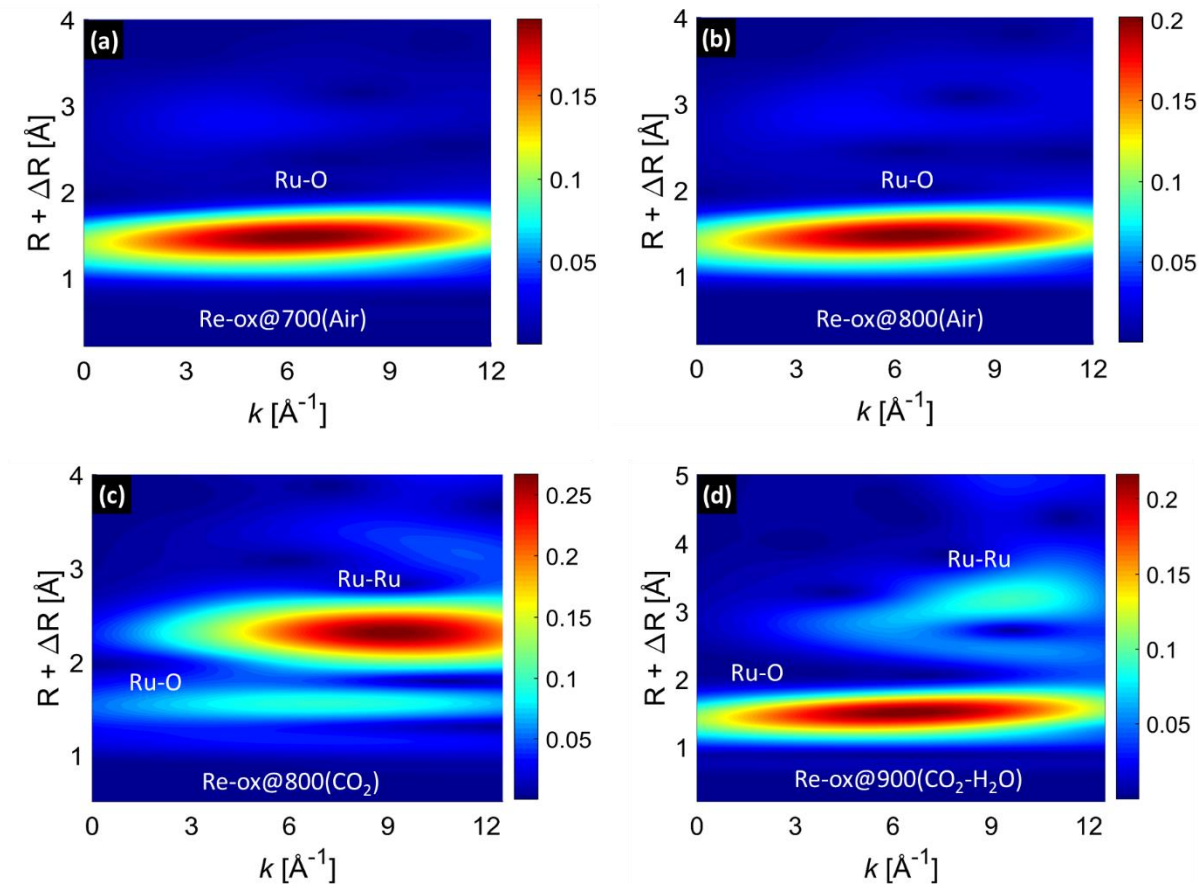

Figure S20: Ex situ Ru K-edge WT of k^3-weighted EXAFS data of $Sm_2Ru_{0.2}Ce_{1.8}O_{7(DRM-800)}$ after re-oxidation in (a, b) air, (c) CO_2, and (d) CO_2/steam mixture at different temperatures. $Sm_2Ru_{0.2}Ce_{1.8}O_7$ was treated at 800 °C for 1 h in a DRM reaction mixture for each experiment. Re-oxidation was performed in air (20 vol% O_2 in N_2), pure CO_2 and a CO_2/steam mixture (10 vol% H_2O) for 1 h.

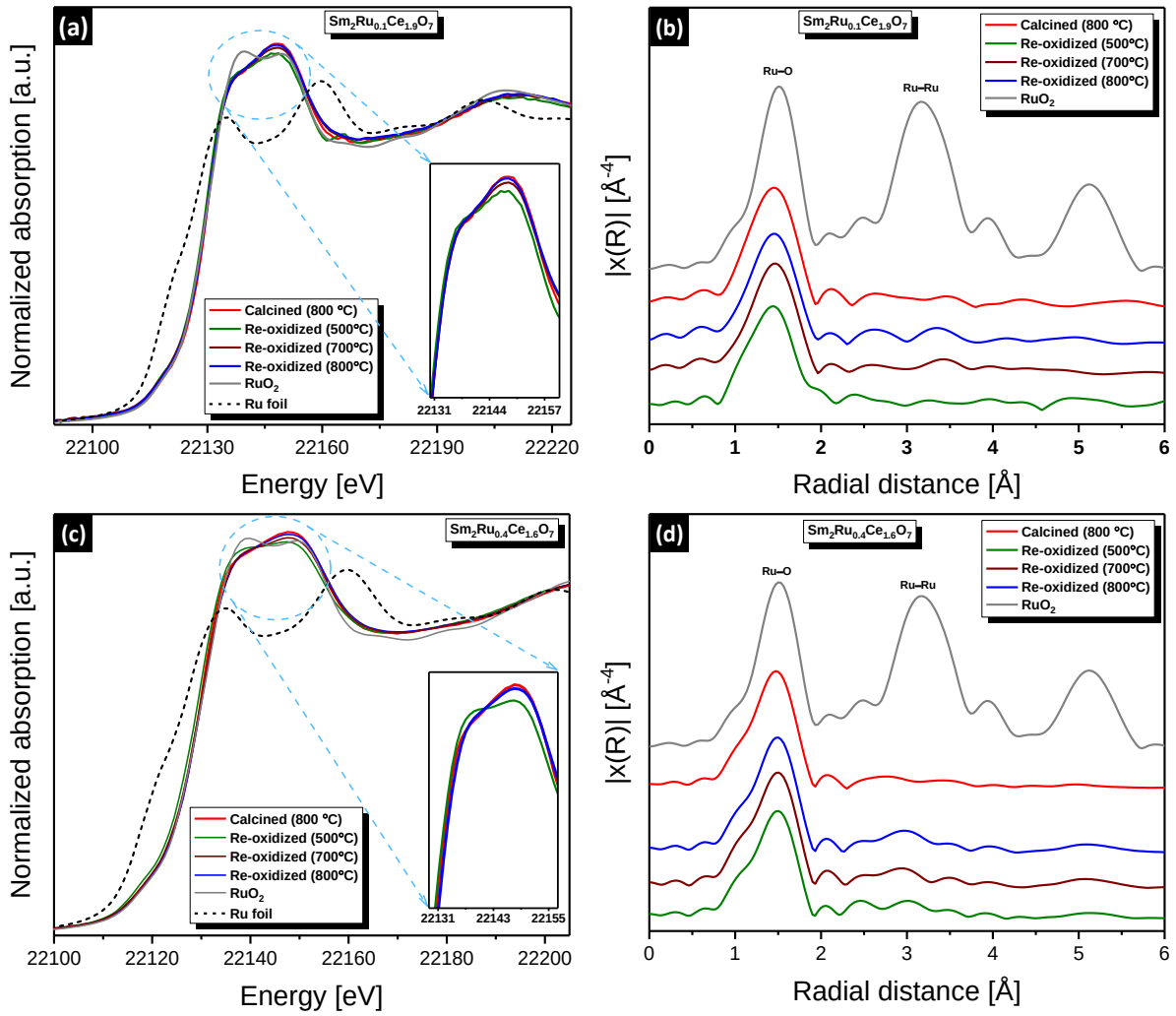

Figure S21: (a, c) Normalized ex situ Ru K-edge XANES spectra and (b, d) Fourier transforms of the k^3-weighted EXAFS data of $Sm_2Ru_xCe_{2-x}O_7$ (x = 0.1, 0.4) treated under different conditions. The materials were treated at 800 °C for 1 h in a DRM mixture. Re-oxidation was performed in air (20 vol% O_2 in N_2) for 1 h (500, 700 and 800 °C).

Probing the reversibility of Ru exsolution under mild oxidizing atmospheres

Having demonstrated the reversibility of the exsolution of Ru and its re-incorporation into the host structure using air as on oxidant, we tested whether milder oxidants such as CO_2 or a mixture of CO_2-steam (10 vol% H_2O) would have the same effect as air. Normalized ex situ Ru K-edge XANES spectra and FT EXAFS functions of $Sm_2Ru_{0.2}Ce_{1.8}O_{7(DRM\text{-}800)}$ after re-oxidation in CO_2 or a CO_2-steam mixture at different temperatures are compared in Figure S22. The re-oxidation of $Sm_2Ru_{0.2}Ce_{1.8}O_{7(DRM\text{-}800)}$ in CO_2 at 800 °C yields a slight shift towards higher energies (22119.9 eV) in the edge position of Ru when compared to the Ru foil (22117.0 eV), suggesting only a partial oxidation of Ru. In contrast, re-oxidation at 800 °C in a mixture of CO_2-steam leads to a marked shift (22128.1 eV) in the edge position of Ru towards higher energies, suggesting that a higher fraction of Ru is oxidized, nevertheless the re-oxidation and dissolution of Ru does not proceed to completion, according to the XANES features which differ considerably form the XANES of the initial solid solution. The incomplete oxidation is further confirmed by FT (Figure S22a) and WT (Figure S22b) analysis of the k^3-weighted EXAFS data showing a peak due to metallic Ru (i.e., Ru-Ru coordination sphere at ca. 2.5 Å). $Sm_2Ru_{0.2}Ce_{1.8}O_{7(DRM\text{-}800)}$ reached an oxidation state close to Ru^{4+} (edge position: 22129.9 eV) after re-oxidation in a CO_2-steam mixture at 900 °C; however, the XANES white line features of the calcined $Sm_2Ru_{0.2}Ce_{1.8}O_7$ were still not fully recovered. Additionally, WT analysis results (Figure S20d) reveal the formation of RuO_2 after re-oxidization in a CO_2-steam mixture at 900 °C owing to the presence of the peak due the Ru-Ru coordination shell at ca. 3Å (Figure S5d).

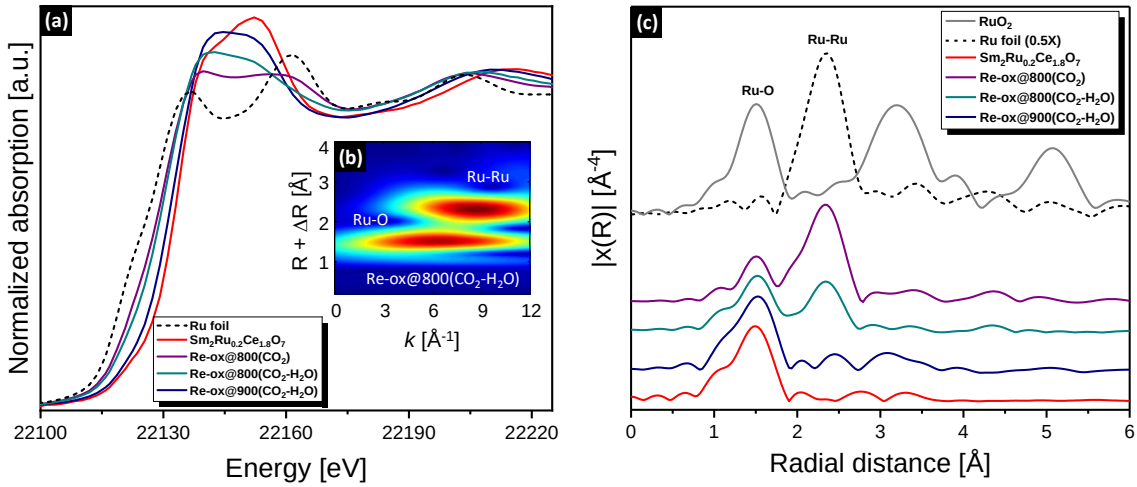

Figure S22: Ex situ Ru K-edge (a) XANES spectra, (b) WT, and (c) FT of the k^3-weighted EXAFS data of $Sm_2Ru_{0.2}Ce_{1.8}O_{7(DRM\text{-}800)}$ after re-oxidation in CO_2 and a mixture of CO_2 and steam. $Sm_2Ru_{0.2}Ce_{1.8}O_7$ was pre-treated at 800 °C for 1 h in a DRM reaction mixture for each experiment. Re-oxidation was performed in pure CO_2 or a CO_2/steam mixture (10 vol% H_2O) for 1 h, respectively.

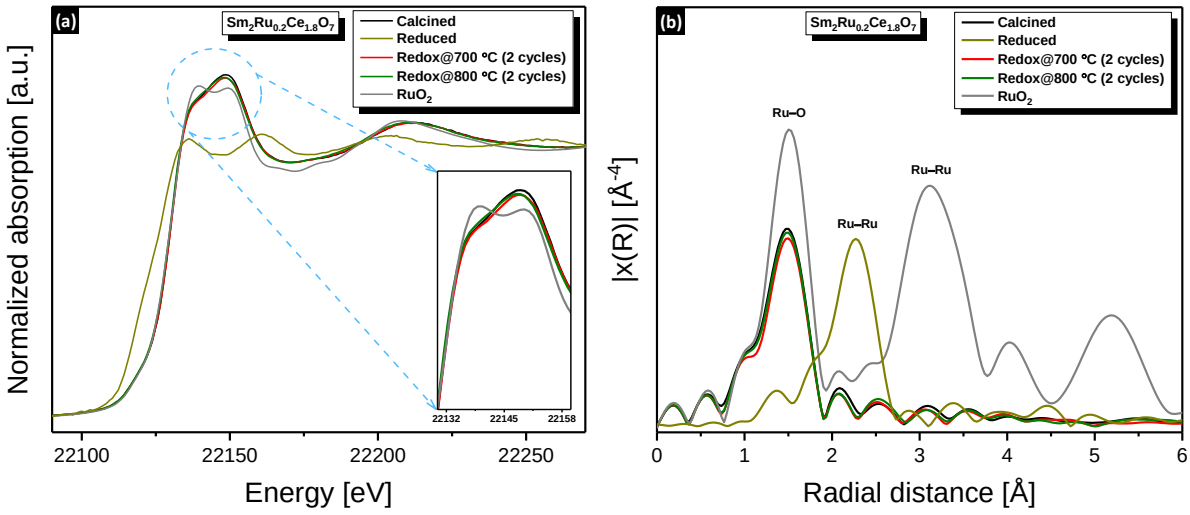

Figure S23: (a) Normalized ex situ Ru K-edge XANES spectra and (b) Fourier transforms of the k^3-weighted EXAFS data of $Sm_2Ru_{0.2}Ce_{1.8}O_7$ after two redox cycles at different temperatures. $Sm_2Ru_{0.2}Ce_{1.8}O_7$ was treated at 800 °C for 1 h in a DRM reaction mixture for each experiment. Re-oxidation was performed in air (20 vol% O_2 in N_2) for 1 h.